Wang Lixian*

Dynamic response analysis of fluid-saturated porous rectangular plates

https://doi.org/10.1515/zna-2020-0179 Received April 28, 2020; accepted September 9, 2020; published online October 21, 2020

Abstract: Based on Biot's model for saturated porous media, the governing equation of fluid-saturated porous rectangular plates is presented, in which the compressibility of solid particles and fluid and the viscosity of pore fluid is taken into account. A series solution is given for simply-supported fluid-saturated porous plates. The accuracy of the solution is validated by degenerating the fluid-saturated porous rectangular plates into single-phase solid rectangular plates. As a numerical example, the free vibration characteristic and the dynamic response under harmonic loads are analysed. The influence of surface infiltration conditions, porosity, pore fluid permeability coefficient and loading frequency on the free vibration frequency is discussed.

Keywords: dynamic response; free vibration; power series method; rectangular plates; saturated porous media.

1 Introduction

Since Biot (1956) [1, 2] put forward the basic equations describing the dynamic characteristics of saturated porous media, the theory of porous media has become the foundation for studying the dynamic characteristics and performing dynamic analysis of saturated porous media, and has been widely used in different engineering of a variety of fields.

To date, research on saturated porous media in the fields of geotechnical engineering, earthquake engineering and geophysical has mainly focused on geotechnical materials whose geometric characteristics are associated with the half-space domain or an infinite horizontal layer, including theoretical analysis and numerical simulation of dynamic responses [3–10] and wave propagation characteristics [11–14]. However, few studies have been focused on flexible structures, such as porous media beams, plates and shell

structures. On the one hand, the behaviour of flexible porous structures is an important issue in biomechanics [15, 16], such as the mechanical analysis of cartilage tissue and the stems of plants. On the other hand, porous materials such as polyurethane foams and fibrous materials have been widely used in the automotive and aerospace industries for damping and sound absorption [17, 18]. Therefore, it is necessary to further study the static and dynamic mechanical behaviours of flexible porous structures.

In terms of fluid-saturated porous plate structures, considering the lateral diffusion of fluid, Taber [19] established the solid-phase and fluid-phase governing equation of the isotropic fluid-saturated porous media based on Biot's model to analyse the dynamic bending of simply supported rectangular porous plates using the Laplace transformation and the perturbation method. Leclaire et al. [20] analysed the transverse vibration problem of rectangular thin plates for four-edge-clamped porous media using the Rayleigh-Ritz method, which takes the effect of fluid viscosity on energy dissipation into account. Based on the research of Theodorakopoulos and Beskos [21] on the bending vibration of porous elastic plates and Biot's theory, Anke and Heinz [22] established the dynamic mathematical model of saturated porous elastic Mindlin plates and gave the principle of virtual work using the deflection, angle and pore stress as basic unknown quantities. Based on the classical theory of homogeneous plates and Biot's stress-strain relations in an isotropic porous medium with a uniform porosity, Feng-xi and Xiao-lin [23] researched the dynamic bending mathematical model of saturated porous elastic plates, and the influence of porosity, tortuosity and permeability on the resonances was studied to determine the condition of maximum damping considering these parameters. Nagler and Schanz [24], using the series approximation method, obtained another plate shear deformation theory of porous material plates. Many studies on the mechanical response of fluid-saturated porous plates used various simplified plate theories, such as classical thin plate theory and Reissner-Mindlin thick plate theory. Rezaei and Saidi [25] presented an exact solution for the free vibration analysis of porous rectangular plates under undrained conditions, and the results show that the effect of coupled fluid-solid deformation may not be disregarded. However, other studies have shown that

^{*}Corresponding author: Wang Lixian, School of Civil Engineering, Lanzhou University of Technology, Langongping Road 287#, Lanzhou 730050, People's Republic of China, E-mail: wangkian@lut.edu.cn

the mechanical quantity cannot be a polynomial of coordinate variables in the thickness direction. In various simplified theories, incompatibility among the fundamental equations can be found, that is, some mechanical quantities can meet only some and not all of the basic equations, and the error will increase greatly with increasing thickness [26].

Based on Biot's model of porous media and threedimensional elastic theory, the dynamic governing equation of fluid-saturated porous rectangular plates is established in this paper. The free vibration and forced vibration responses of simply supported fluid-saturated porous rectangular plates are researched. The influence of the surface infiltration conditions, porosity, pore fluid permeability coefficient and loading frequency parameters on the free vibration frequency, the solid skeleton stress, the pore fluid pressure, the solid skeleton displacement and pore fluid displacement of plates are analysed *via* numerical examples.

2 The governing equation of fluid-saturated porous rectangular plates

A rectangular plate occupying the region $[0, L_1] \times [0, L_2] \times [-H/$ 2, H/2] in the unstressed reference configuration is described in rectangular Cartesian coordinates x_i (i = 1, 2, 3). Based on Biot's model of porous media, the basic equations of homogeneous saturated porous media are as follows.

The constitutive equations for a fluid-saturated porous media are

$$\sigma_{ii} = \lambda \varepsilon_{kk} \delta_{ii} + 2\mu \varepsilon_{ii} - \alpha p \delta_{ii} \tag{1}$$

$$p = M\zeta - \alpha M \varepsilon_{kk} \tag{2}$$

The strain tensor for infinitesimal deformations is related to the displacements u_i by

$$\varepsilon_{ij} = \frac{1}{2} \left(u_{i,j} + u_{j,i} \right) \tag{3}$$

The equilibrium equations in the absence of a body force are

$$\sigma_{ij,j} = \rho \ddot{u}_i + \rho_f \ddot{w}_i \tag{4}$$

$$-p_{,i} = \rho_f \ddot{u}_i + m \ddot{w}_i + b \dot{w}_i \tag{5}$$

where σ_{ii} and p are the total stress components and pore fluid pressure (i, j = 1, 2, 3), respectively. u_i and w_i are the displacement components of the solid skeleton and pore fluid, that is $e = u_{i,i}$, and $\zeta = -w_{i,i}$. λ and μ are the Lame constants and ε_{ii} is the strain vector of the solid skeleton. b

is a parameter accounting for internal friction due to the relative motion between the solid and the pore fluid and $b = \eta/k_f$, where k_f is the dynamic permeability and η is the viscosity of the fluid. α and M are the Biot parameters considering compressibility of the two-phase material, and $\alpha = 1 - K/K_s$, $1/M = (\alpha - n)/K_s + n/K_f$, where K, K_s and K_f are the bulk modulus of the solid skeleton, solid particles and pore fluid, respectively, while n is the soil porosity. ρ is the total density of the saturated soil and can be represented by $\rho = (1 - n)\rho_s + n\rho_f$, where ρ_s and ρ_f are the densities of the solid phase and liquid phase, respectively. m is a parametric representation related to the mass density of the pore fluid and pore geometry features $m = \rho_f/n$.

Combining Eqs. (1)–(5), the governing equations of the dynamic response of the saturated media can be obtained as

$$\mu \nabla^2 u + (\lambda + \mu + \alpha^2 M) \nabla e - \alpha M \nabla \zeta = \rho \ddot{u} + \rho_f \ddot{w}$$
 (6)

$$\nabla \left(\alpha Me - M\zeta\right) = \left(\rho_f \ddot{u} + m\ddot{w}\right) + b\dot{w} \tag{7}$$

Considering the simply supported boundary conditions, that is

$$\sigma_{11} = 0, u_2 = u_3 = 0, w_2 = w_3 = 0, \text{ at } x_1 = 0, L_1;$$

 $\sigma_{22} = 0, u_1 = u_3 = 0, w_1 = w_3 = 0, \text{ at } x_2 = 0, L_2.$ (8)

3 The exact solution for fluid-saturated porous rectangular plates

A solution for the displacement field in the fluid-saturated porous rectangular plate is sought in the form.

$$u_{1} = \sum_{m_{1}=0, n_{1}=0}^{\infty} U_{1}(x_{3}) \cos \frac{m_{1}\pi x_{1}}{L_{1}} \sin \frac{n_{1}\pi x_{2}}{L_{2}} e^{iwt},$$

$$w_{1} = \sum_{m_{1}=0, n_{1}=0}^{\infty} W_{1}(x_{3}) \cos \frac{m_{1}\pi x_{1}}{L_{1}} \sin \frac{n_{1}\pi x_{2}}{L_{2}} e^{iwt}$$

$$u_{2} = \sum_{m_{1}=0, n_{1}=0}^{\infty} U_{2}(x_{3}) \sin \frac{m_{1}\pi x_{1}}{L_{1}} \cos \frac{n_{1}\pi x_{2}}{L_{2}} e^{iwt},$$

$$w_{2} = \sum_{m_{1}=0, n_{1}=0}^{\infty} W_{2}(x_{3}) \sin \frac{m_{1}\pi x_{1}}{L_{1}} \cos \frac{n_{1}\pi x_{2}}{L_{2}} e^{iwt}$$

$$u_{3} = \sum_{m_{1}=0, n_{1}=0}^{\infty} U_{3}(x_{3}) \sin \frac{m_{1}\pi x_{1}}{L_{1}} \sin \frac{n_{1}\pi x_{2}}{L_{2}} e^{iwt},$$

$$w_{3} = \sum_{m_{1}=0, n_{1}=0}^{\infty} W_{3}(x_{3}) \sin \frac{m_{1}\pi x_{1}}{L_{1}} \sin \frac{n_{1}\pi x_{2}}{L_{2}} e^{iwt}$$

where ω denotes the angular frequency. Assume that $\xi_1 = m_1 \pi / L_1$, $\xi_2 = n_1 \pi / L_2$ and that m_1 and n_1 are positive integers. The chosen displacement field described by Eq. (9) by Eq. (8) at simply supported boundaries. Substituting Eqs.

satisfies the homogeneous boundary conditions described (3) and (9) into the constitutive equation of Eq. (1), the stresses can be given in terms of displacements as

$$\begin{cases} \sigma_{11} = \sum_{m_1, n_1} \left[-(\lambda + 2\mu + \alpha^2 M) \, \xi_1 U_1 - \alpha M \xi_1 W_1 - (\lambda + \alpha^2 M) \, \xi_2 U_2 - \alpha M \xi_2 W_2 + (\lambda + \alpha^2 M) \, U_3' + \alpha M W_3' \right] \sin \xi_1 x_1 \sin \xi_2 x_2 e^{i\omega t} \\ \sigma_{22} = \sum_{m_1, n_1} \left[-(\lambda + \alpha^2 M) \, \xi_1 U_1 - \alpha M \xi_1 W_1 - (\lambda + 2\mu + \alpha^2 M) \, \xi_2 U_2 - \alpha M \xi_2 W_2 + (\lambda + \alpha^2 M) \, U_3' + \alpha M W_3' \right] \sin \xi_1 x_1 \sin \xi_2 x_2 e^{i\omega t} \\ \sigma_{33} = \sum_{m_1, n_1} \left[-(\lambda + \alpha^2 M) \, \xi_1 U_1 - \alpha M \xi_1 W_1 - (\lambda + \alpha^2 M) \, \xi_2 U_2 - \alpha M \xi_2 W_2 + (\lambda + 2\mu + \alpha^2 M) \, U_3' + \alpha M W_3' \right] \sin \xi_1 x_1 \sin \xi_2 x_2 e^{i\omega t} \\ \sigma_{12} = \sum_{m_1, n_1} \mu \left(\xi_2 U_1 + \xi_1 U_2 \right) \cos \xi_1 x_1 \cos \xi_2 x_2 e^{i\omega t} \\ \sigma_{13} = \sum_{m_1, n_1} \mu \left(U_1' + \xi_1 U_3 \right) \cos \xi_1 x_1 \sin \xi_2 x_2 e^{i\omega t} \\ \sigma_{23} = \sum_{m_1, n_1} \mu \left(U_2' + \xi_2 U_3 \right) \sin \xi_1 x_1 \cos \xi_2 x_2 e^{i\omega t} \\ \sigma_{23} = \sum_{m_1, n_1} \mu \left(U_2' + \xi_2 U_3 \right) \sin \xi_1 x_1 \cos \xi_2 x_2 e^{i\omega t} \\ p = \sum_{m_1, n_1} (\alpha M \xi_1 U_1 + M \xi_1 W_1 + \alpha M \xi_2 U_2 + M \xi_2 W_2 - \alpha M U_3' - M W_3') \sin \xi_1 x_1 \cos \xi_2 x_2 e^{i\omega t} \end{cases}$$
(10)

(11d)

(11f)

where a prime denotes differentiation with respect to x_3 . Substituting Eq. (9) into Eqs. (6) and (7), the following coupled system of second-order ordinary differential equations can be obtained:

$$\begin{split} \left[\rho\omega^{2} - \left(\xi_{1}^{2} + \xi_{2}^{2}\right)\mu - \left(\lambda + \mu + \alpha^{2}M\right)\right]\xi_{1}^{2}U_{1} + \mu U_{1}^{''} \\ + \left(\rho_{f}\omega^{2} - \alpha M\xi_{1}^{2}\right)W_{1} - \left(\lambda + \mu + \alpha^{2}M\right)\xi_{1}\xi_{2}U_{2} - \alpha M\xi_{1}\xi_{2}W_{2} \\ + \left(\lambda + \mu + \alpha^{2}M\right)\xi_{1}U_{3}^{'} + \alpha M\xi_{1}W_{3}^{'} = 0 \end{split} \tag{11a}$$

$$\begin{split} &-\left(\lambda + \mu + \alpha^{2}M\right)\xi_{1}\xi_{2}U_{1} - \alpha M\xi_{1}\xi_{2}W_{1} \\ &+ \left[\rho w^{2} - \left(\xi_{1}^{2} + \xi_{2}^{2}\right)\mu - \left(\lambda + \mu + \alpha^{2}M\right)\xi_{2}^{2}\right]U_{2} + \mu U_{2}^{''} \\ &+ \left(\rho_{f}w^{2} - \alpha M\xi_{2}^{2}\right)W_{2} + \left(\lambda + \mu + \alpha^{2}M\right)\xi_{2}U_{3}^{'} + \alpha M\xi_{2}W_{3}^{'} = 0 \end{split} \tag{11b}$$

$$- (\lambda + \mu + \alpha^{2}M) \xi_{1}U_{1}^{'} - \alpha M \xi_{1}W_{1}^{'} - (\lambda + \mu + \alpha^{2}M) \xi_{2}U_{2}^{'}$$

$$- \alpha M \xi_{2}W_{2}^{'} + \left[\rho\omega^{2} - \mu(\xi_{1}^{2} + \xi_{2}^{2})\right] U_{3} + (\lambda + 2\mu + \alpha^{2}M) U_{3}^{''}$$

$$+ \rho_{f}\omega^{2}W_{3} + \alpha M W_{3}^{''} = 0$$
(11c)

$$(\rho_f \omega^2 - \alpha M \xi_1^2) U_1 + (m\omega^2 - b\omega i - M \xi_1^2) W_1 - \alpha M \xi_1 \xi_2 U_2 - M \xi_1 \xi_2 W_2 + \alpha M \xi_1 U_3' + M \xi_1 W_3' = 0$$

$$-\alpha M \xi_1 \xi_2 U_1 - M \xi_1 \xi_2 W_1 + \left(\rho_f \omega^2 - \alpha M \xi_2^2 \right) U_2$$

$$+ \left(m \omega^2 - b \omega i - M \xi_2^2 \right) W_2 + \alpha M \xi_2 U_3^{'} + M \xi_2 W_3^{'} = 0$$
(11e)

$$-\alpha M \xi_1 U_1^{'} - M \xi_1 W_1^{'} - \alpha M \xi_2 U_2^{'} - M \xi_2 W_2^{'} + \rho_f \omega^2 U_3 + \alpha M U_3^{''}$$

+ $(m\omega^2 - b\omega i) W_3 + M W_3^{''} = 0$

The power series method is used to obtain the solution for Eq. (11). According to a general method, we assume a power series solution for the displacement functions $U_i(x_3)$ and $W_i(x_3)$ as

$$U_{i}(x_{3}) = \sum_{\beta=0}^{\infty} \tilde{U}_{i}^{(\beta)} x_{3}^{\beta}, W_{i}(x_{3}) = \sum_{\beta=0}^{\infty} \tilde{W}_{i}^{(\beta)} x_{3}^{\beta}$$
(12)

Substituting Eq. (12) into Eq. (11) yields the following coupled recurrence algebraic relations:

$$\widetilde{W}_{1}^{(\beta+1)} = -\frac{\rho_{f}\omega^{2}}{m\omega^{2} - b\omega i} \widetilde{U}_{1}^{(\beta+1)} + \frac{\rho_{f}\omega^{2}\xi_{1}}{(m\omega^{2} - b\omega i)(\beta+1)} \widetilde{U}_{3}^{(\beta)} + \frac{\xi_{1}}{\beta+1} \widetilde{W}_{3}^{(\beta)}$$
(13a)

$$\widetilde{W}_{2}^{\left(\beta+1\right)} = -\frac{\rho_{f}\omega^{2}}{m\omega^{2} - b\omega i} \widetilde{U}_{2}^{\left(\beta+1\right)} + \frac{\rho_{f}\omega^{2}\xi_{2}}{(m\omega^{2} - b\omega i)(\beta+1)} \widetilde{U}_{3}^{\left(\beta\right)} + \frac{\xi_{2}}{\beta+1} \widetilde{W}_{3}^{\left(\beta\right)}$$

$$(13b)$$

$$\begin{split} \widetilde{W}_{3}^{(\beta+1)} &= \frac{\alpha M \left(\xi_{1}^{2} + \xi_{2}^{2}\right) - \rho_{f}\omega^{2}}{M\xi_{1}(\beta+1)} \; \widetilde{U}_{1}^{(\beta)} \\ &+ \frac{\rho_{f}\omega^{2}\xi_{2} - \alpha\xi_{2}(m\omega^{2} - b\omega i)}{\rho_{f}\omega^{2}(\beta+1)} \; \widetilde{W}_{2}^{(\beta)} \\ &+ \frac{\left(\alpha M\xi_{2}^{2} - \rho_{f}\omega^{2}\right)\left(m\omega^{2} - b\omega i\right) + \rho_{f}\omega^{2}M\xi_{1}^{2}}{\rho_{f}\omega^{2}M\xi_{1}(\beta+1)} \; \widetilde{W}_{1}^{(\beta)} \\ &- \alpha \widetilde{U}_{3}^{(\beta+1)} \end{split}$$

$$(13c)$$

$$\begin{split} \widetilde{U}_{1}^{(\beta+2)} &= \frac{\left(\alpha \rho_{f} - \rho\right) \omega^{2} + \left(\xi_{1}^{2} + \xi_{2}^{2}\right) (\lambda + 2\mu)}{\mu(\beta + 2) (\beta + 1)} \, \widetilde{U}_{1}^{(\beta)} \\ &- \frac{(\lambda + \mu) \, \xi_{1} \xi_{2} (m\omega^{2} - b\omega i)}{\mu \rho_{f} \omega^{2} (\beta + 2) (\beta + 1)} \, \widetilde{W}_{2}^{(\beta)} \\ &+ \frac{\left[\alpha \rho_{f} \omega^{2} + (\lambda + \mu) \xi_{2}^{2}\right] (m\omega^{2} - b\omega i) - \left(\rho_{f} \omega^{2}\right)^{2}}{\mu \rho_{f} \omega^{2} (\beta + 2) (\beta + 1)} \, \widetilde{W}_{1}^{(\beta)} \\ &- \frac{(\lambda + \mu) \, \xi_{1}}{\mu (\beta + 2)} \, \widetilde{U}_{3}^{(\beta+1)} \end{split}$$
(13d)

$$\begin{split} \widetilde{U}_{2}^{\,(\beta+2)} &= \frac{\xi_{2} \Big[\, \big(\lambda + 2 \mu \big) \big(\xi_{1}^{2} + \xi_{2}^{2} \big) + \big(\alpha \rho_{f} - \rho \big) \, \omega^{2} \big]}{\mu \xi_{1} (\beta + 2) \, (\beta + 1)} \, \widetilde{U}_{1}^{\,(\beta)} \\ &- \frac{(\lambda + \mu) \xi_{2}}{\mu (\beta + 2)} \, \widetilde{U}_{3}^{\,(\beta+1)} \\ &+ \frac{(m \omega^{2} - b \omega i) \, \xi_{2} \Big[\big(\alpha \rho_{f} - \rho \big) \omega^{2} + \big(\xi_{1}^{2} + \xi_{2}^{2} \big) \, \mu + (\lambda + \mu) \, \xi_{2}^{2} \Big]}{\mu \rho_{f} \omega^{2} \xi_{1} \, (\beta + 2) \, (\beta + 1)} \, \widetilde{W}_{1}^{\,(\beta)} \\ &- \frac{(m \omega^{2} - b \omega i) \big[\rho \omega^{2} + \mu \big(\xi_{1}^{2} + \xi_{2}^{2} \big) + (\lambda + \mu) \, \xi_{2}^{2} \big] - \big(\rho_{f} \omega^{2} \big)^{2}}{\mu \rho_{f} \omega^{2} \, (\beta + 2) \, (\beta + 1)} \, \widetilde{W}_{2}^{\,(\beta)} \end{split}$$

$$\begin{split} \widetilde{U}_{3}^{\left(\beta+2\right)} &= \frac{\left(\lambda+\mu\right)\xi_{1}}{\left(\lambda+2\mu\right)\left(\beta+2\right)}\,\widetilde{U}_{1}^{\left(\beta+1\right)} + \frac{\left(\lambda+\mu\right)\xi_{2}}{\left(\lambda+2\mu\right)\left(\beta+2\right)}\,\widetilde{U}_{2}^{\left(\beta+1\right)} \\ &\quad + \frac{\left(\alpha\rho_{f}-\rho\right)\omega^{2}+\mu\left(\xi_{1}^{2}+\xi_{2}^{2}\right)}{\left(\lambda+2\mu\right)\left(\beta+2\right)\left(\beta+1\right)}\,\widetilde{U}_{3}^{\left(\beta\right)} \\ &\quad + \frac{\alpha\left(m\omega^{2}-b\omega i\right)-\rho_{f}\omega^{2}}{\left(\lambda+2\mu\right)\left(\beta+2\right)\left(\beta+1\right)}\,\widetilde{W}_{3}^{\left(\beta\right)} \end{split}$$

(13f)

Clearly, the recurrence relations described in Eq. (13) are evaluated successively for β = 0, 1, ..., to obtain $\tilde{U}_i^{(\beta)}$ and $\tilde{W}_i^{(\beta)}$ In terms of the eight arbitrary constants $\tilde{U}_1^{(0)}$, $\tilde{W}_1^{(0)}$, $\tilde{W}_2^{(0)}$, $\tilde{U}_3^{(0)}$, $\tilde{W}_3^{(0)}$, $\tilde{U}_1^{(1)}$, $\tilde{U}_2^{(1)}$, and $\tilde{U}_3^{(1)}$ and the angular frequency ω as

$$\begin{split} \widetilde{U}_{i}^{\left(\beta\right)} &= A_{i1}^{\left(\beta\right)}(\omega)\widetilde{U}_{1}^{(0)} + A_{i2}^{\left(\beta\right)}(\omega)\widetilde{W}_{1}^{(0)} \\ &+ A_{i3}^{\left(\beta\right)}(\omega)\widetilde{W}_{2}^{(0)} + A_{i4}^{\left(\beta\right)}(\omega)\widetilde{U}_{3}^{(0)} + A_{i5}^{\left(\beta\right)}(\omega)\widetilde{W}_{3}^{(0)} \\ &+ A_{i6}^{\left(\beta\right)}(\omega)\widetilde{U}_{1}^{(1)} + A_{i7}^{\left(\beta\right)}(\omega)\widetilde{U}_{2}^{(1)} + A_{i8}^{\left(\beta\right)}(\omega)\widetilde{U}_{3}^{(1)} \end{split} \tag{14a}$$

$$\begin{split} \widetilde{W}_{i}^{(\beta)} &= B_{i1}^{(\beta)}(\omega)\widetilde{U}_{1}^{(0)} + B_{i2}^{(\beta)}(\omega)\widetilde{W}_{1}^{(0)} + B_{i3}^{(\beta)}(\omega)\widetilde{W}_{2}^{(0)} \\ &+ B_{i4}^{(\beta)}(\omega)\widetilde{U}_{3}^{(0)} + B_{i5}^{(\beta)}(\omega)\widetilde{W}_{3}^{(0)} + B_{i6}^{(\beta)}(\omega)\widetilde{U}_{1}^{(1)} \\ &+ B_{i7}^{(\beta)}(\omega)\widetilde{U}_{2}^{(1)} + B_{i8}^{(\beta)}(\omega)\widetilde{U}_{3}^{(1)} \end{split} \tag{14b}$$

Here, $A_{ij}^{(\beta)}(\omega)$ and $B_{ij}^{(\beta)}(\omega)$ are known polynomials in ω and they are determined by the recurrence formula in Eq. (13).

Substituting Eq. (14) into Eq. (12) gives the rewritten displacement expression as

$$\begin{split} U_{i}(x_{3}) &= A_{i1}(x_{3})\widetilde{U}_{1}^{(0)} + A_{i2}(x_{3})\widetilde{W}_{1}^{(0)} + A_{i3}(x_{3})\widetilde{W}_{2}^{(0)} \\ &+ A_{i4}(x_{3})\widetilde{U}_{3}^{(0)} + A_{i5}(x_{3})\widetilde{W}_{3}^{(0)} + A_{i6}(x_{3})\widetilde{U}_{1}^{(1)} \\ &+ A_{i7}(x_{3})\widetilde{U}_{2}^{(1)} + A_{i8}(x_{3})\widetilde{U}_{3}^{(1)} \end{split} \tag{15a}$$

$$W_{i}(x_{3}) = B_{i1}(x_{3})\widetilde{U}_{1}^{(0)} + B_{i2}(x_{3})\widetilde{W}_{1}^{(0)} + B_{i3}(x_{3})\widetilde{W}_{2}^{(0)} + B_{i4}(x_{3})\widetilde{U}_{3}^{(0)} + B_{i5}(x_{3})\widetilde{W}_{3}^{(0)} + B_{i6}(x_{3})\widetilde{U}_{1}^{(1)}$$
(15b)
+ $B_{i7}(x_{3})\widetilde{U}_{2}^{(1)} + B_{i8}(x_{3})\widetilde{U}_{3}^{(1)}$

where $A_{ij}(x_3) = \sum_{\beta=0}^{\infty} A_{ij}^{(\beta)} x_3^{\beta}$, and $B_{ij}(x_3) = \sum_{\beta=0}^{\infty} B_{ij}^{(\beta)} x_3^{\beta}$. The degree of each of the polynomials increases as more terms are retained in the series expansion in Eq. (12).

Substituting the expressions of displacement in Eq. (15) into the stress components in Eq. (10) represented by displacement yields the following expression of stress:

$$S = Q_{ij}\tilde{U} \tag{16}$$

where $\mathbf{S} = \begin{bmatrix} \sigma_{33} & \sigma_{13} & \sigma_{23} & p \end{bmatrix}^T$, $\widetilde{\mathbf{U}} = \begin{bmatrix} \widetilde{U}_1^{(0)} & \widetilde{W}_1^{(0)} & \widetilde{U}_2^{(0)} \\ \widetilde{W}_2^{(0)} & \widetilde{U}_3^{(0)} & \widetilde{U}_1^{(1)} & \widetilde{U}_3^{(1)} \end{bmatrix}^T$, and the matrix of coefficients \mathbf{Q}_{ij} is a 4×8 matrix for each i,j given in Appendix A.

At this point, a series solution of the displacement and stress components are obtained.

3.1 The free vibration of fluid-saturated porous rectangular plates

If the upper and lower surfaces of the plate are both freely permeable, and the boundary conditions for the free vibration are:

$$\sigma_{33} = 0, \sigma_{13} = \sigma_{23} = 0, p = 0 \text{ at } x_3 = -H/2$$

 $\sigma_{33} = 0, \sigma_{13} = \sigma_{23} = 0, p = 0 \text{ at } x_3 = H/2$ (17)

Therefore, substituting Eq. (16) into the boundary conditions in Eq. (17) yields the frequency equation in matrix form:

$$Q_{ii}(x_3)\widetilde{U}=0 (18)$$

where $\mathbf{Q}_{ii}(x_3)$ is an 8×8 matrix and given in Appendix B.

If the upper and lower surfaces of the plate are impermeable, the boundary conditions for the free vibration change to be:

$$\sigma_{33} = 0, \sigma_{13} = \sigma_{23} = 0, w_3 = 0 \text{ at } x_3 = -H/2$$

 $\sigma_{33} = 0, \sigma_{13} = \sigma_{23} = 0, w_3 = 0 \text{ at } x_3 = H/2$
(19)

Similarly, Eqs. (15b), (16) and (19) can obtain the matrix form of Eq. (20):

$$G_{ii}(x_3)\widetilde{U}=0 \tag{20}$$

where $G_{ii}(x_3)$ is an 8×8 matrix and given in Appendix C.

The left coefficient determinant of the above equation needs to be set to zero to ensure that a nontrivial solution of Eq. (18) or Eq. (20) exists. Thus, the free vibration frequency of fluid-saturated porous rectangular plates can be obtained if the upper or lower surfaces are either freely permeable or completely impermeable.

3.2 The forced vibration of fluid-saturated porous rectangular plates

Since an arbitrary load function can be expanded as a double Fourier series in x_1 and x_2 , considering the upper and lower surfaces of the plate to be freely permeable, the boundary conditions for the forced vibration with the harmonic load can be expressed as:

$$\sigma_{33} = q e^{i\omega t} \sin \xi_1 x_1 \sin \xi_2 x_2, \sigma_{13} = \sigma_{23} = 0, p = 0 \text{ at } x_3 = -H/2$$

$$\sigma_{33} = 0, \sigma_{13} = \sigma_{23} = 0, p = 0 \text{ at } x_3 = -H/2$$

(21)

where q is the amplitude of the normal loads applied on the top surfaces.

Eqs. (16) and (21) can be combined to obtain

$$Q_{ii}(x_3)\widetilde{U} = P \tag{22}$$

where $P = \begin{bmatrix} -q & 0 & 0 & 0 & 0 & 0 & 0 \end{bmatrix}^T$ is a vector of length 8. If the upper and lower surfaces of the plate are impermeable, the boundary conditions for the forced vibration are:

$$\sigma_{33} = qe^{i\omega t}\sin \xi_1 x_1 \sin \xi_2 x_2, \sigma_{13} = \sigma_{23} = 0, w_3 = 0 \text{ at } x_3 = -H/2$$

 $\sigma_{33} = 0, \sigma_{13} = \sigma_{23} = 0, w_3 = 0 \text{ at } x_3 = -H/2$

(23)

Similarly, Eq. (24) can be obtained:

$$G_{ij}(x_3)\widetilde{U} = P$$
 (24)

After determining the constants $\tilde{U}_1^{(0)}$, $\tilde{W}_1^{(0)}$, $\tilde{W}_2^{(0)}$, $\tilde{U}_3^{(0)}$, $\tilde{W}_3^{(0)},~\tilde{U}_1^{(1)},~\tilde{U}_2^{(1)},$ and $\tilde{U}_3^{(1)}$ with Eq. (22) or Eq. (24), the transient response of fluid-saturated porous rectangular plates with harmonic load can be computed by combining Eqs. (15) and (16).

4 Results and discussion

4.1 Results validation

To verify the validity of the presented solution in this paper, the fluid-saturated porous rectangular plates are degenerated into single-phase solid rectangular plates by ignoring the pore fluid pressure p and setting n = 0, $\rho_f = 0$ and $\eta = 0$. Then, Eq. (18) transforms into

$$Q'_{ii}(x_3)\tilde{U}' = 0$$
 (25)

where $Q_{ij}^{'}(x_3)$ is a 6×6 matrix and given in Appendix D. $\widetilde{U}^{'}=\left[\begin{array}{cccc}\widetilde{U}_1^{(0)}&\widetilde{U}_2^{(0)}&\widetilde{U}_3^{(0)}&\widetilde{U}_1^{(1)}&\widetilde{U}_2^{(1)}&\widetilde{U}_3^{(1)}\end{array}\right]^T$.

The parameters selected for the numerical simulation of a fluid-saturated porous rectangular plate are as follows [24]:

$$E = 1.44 \times 10^{10} \text{ Pa}, v = 0.2, \rho_s = 2.458 \text{ kg/m}^3,$$

 $\rho_f = 1.000 \text{ kg/m}^3, K_s = 3.6 \times 10^{10} \text{ pa}, L_1 = L_2 = 1 \text{ m},$
 $K_f = 3.3 \times 10^{10} \text{ pa}, n = 0.19 \text{ and } H = 0.1 \text{ m}$

where E is Young's modulus and ν is Poisson's ratio.

The dimensionless fundamental frequencies $\overline{\omega}$ = $\frac{\omega L_1^2}{H} \sqrt{\frac{\rho}{E}}$ obtained from Eq. (25) are given in Table 1. The listed values in Table 1 indicate that our results are in excellent agreement with those presented by Senthil and Bara [27]. We have also listed the natural frequencies computed from the three plate theories in Table 1 to compare the exact results with those obtained from classical plate theory (CPT) [28], first-order shear deformation theory (FSDT) [29] and third-order shear deformation theory (TSDT) [30]. The comparative results show the validity of the proposed algorithm.

4.2 Free vibration

To analyse the influence of the surface infiltration conditions on the frequency of the fluid-saturated porous rectangular plates, the above calculation parameters are adopted to calculate the natural frequencies of plates according to Eqs. (18) and (20), and the finite series truncated term is β = 10. The boundary conditions on the upper and lower surfaces are permeable and completely impermeable, respectively. The results are listed in Table 2, showing

Table 1: Comparison of exact natural frequencies with natural frequencies from the literature with 10 terms in the series solution.

Theory	$\overline{\omega}_{1,1}^{(1)}$	$\overline{\omega}_{1,1}^{(2)}$	$\overline{\omega}_{1,1}^{(3)}$
$L_1/H = 10$			
Present analysis	5.7762	27.546	46.498
Senthil S.Vel [27]	5.7769	27.554	46.503
CPT [28]	5.9248	27.554	46.574
FSDT [29]	5.7693	27.554	46.574
TSDT [30]	5.7317	27.554	46.574

Table 2: Natural frequencies of the fluid-saturated porous rectangular plates with permeable and completely impermeable upper and lower surfaces.

$L_1/H=10$	$\overline{\omega}_{1,1}^{(1)}$	$\overline{\omega}_{1,1}^{(2)}$	$\overline{\omega}_{1,1}^{(3)}$	$\overline{\omega}_{1,1}^{(4)}$	$\overline{\omega}_{1,1}^{(5)}$
Free permeable	4.1329	28.1538	192.3431	310.9472	380.5576
Completely impermeable	6.4177	41.8564	192.2777	309.8759	379.9566

that the surface infiltration conditions have a great influence on the basic natural frequency of vibration but have little impact on the higher-order frequency.

The natural frequencies are calculated according to Eqs. (18) and (20) under different porosities, permeability coefficients and boundary permeability conditions. The results are listed in Tables 3-6. Tables 3 and 4 show that the natural frequencies of the fluid-saturated porous plates increase with the permeability coefficient whether the upper and lower surfaces are permeable or completely impermeable. Furthermore, the permeability coefficient has more of an influence on the natural frequencies if the upper and lower surfaces are freely permeable. Tables 5 and 6 indicate that the natural frequencies decrease with increasing porosity, whether the upper and lower surfaces are permeable or completely impermeable, and that the porosity has a greater influence on the natural frequencies. These phenomena result from the effect of deformation coupling between the solid and fluid.

4.3 Harmonic vibration

The response of the fluid-saturated porous rectangular plates under the dynamic load is analysed with the harmonic load q = 1000 pa. The results for the forced vibration are plotted in Figure 1 with the harmonic load and forcing frequencies $\overline{w} = 5$, 10, 20 and 50. The solid skeleton stress, the pore fluid pressure, the solid skeleton displacement and the pore fluid displacement of the fluid-saturated porous rectangular plates decrease with increasing forcing

Table 3: Variations in the natural frequencies of fluid-saturated porous rectangular plates with k_r under freely permeable conditions.

$L_1/H=10$	$\overline{\omega}_{1,1}^{(1)}$	$\overline{\omega}_{1,1}^{(2)}$	$\overline{\omega}_{1,1}^{(3)}$	$\overline{\omega}_{1,1}^{(4)}$	$\overline{\omega}_{1,1}^{(5)}$
$k_f = 1 \times 10^{-11}$					
$k_f = 5 \times 10^{-11}$	3.4294	28.1538	192.3369	310.9306	380.5649
$k_f = 1 \times 10^{-10}$	3.7030	28.1538	192.3374	310.9448	380.5650
$k_f = 5 \times 10^{-10}$	5.1163	28.1551	192.3376	310.9455	380.5650
$k_f = 1 \times 10^{-9}$					
$k_f = 5 \times 10^{-9}$	6.1392	28.2661	192.3462	310.9827	380.5691

Table 4: Variations in the natural frequencies of fluid-saturated porous rectangular plates with k_f under freely impermeable conditions.

$L_1/H=10$	$\overline{\omega}_{1,1}^{(1)}$	$\overline{\omega}_{1,1}^{(2)}$	$\overline{\omega}_{1,1}^{(3)}$	$\overline{\omega}_{1,1}^{(4)}$	$\overline{\omega}_{1,1}^{(5)}$
$k_f = 1 \times 10^{-11}$	6.3857	41.8547	192.2755	309.8590	379.9485
$k_f = 5 \times 10^{-11}$	6.4143	41.8562	192.2759	309.8705	379.9533
$k_f = 1 \times 10^{-10}$	6.4158	41.8562	192.2768	309.8790	379.9553
$k_f = 5 \times 10^{-10}$	6.4314	41.8563	192.2769	309.8795	379.9564
$k_f = 1 \times 10^{-9}$	6.4579	41.8564	192.2772	309.8810	379.9570
$k_f = 5 \times 10^{-9}$	6.4646	41.8568	192.2860	309.9202	379.9594

Table 5: Variations in the natural frequencies of fluid-saturated porous rectangular plates with *n* under freely permeable conditions.

$L_1/H=10$	$\overline{\omega}_{1,1}^{(1)}$	$\overline{\omega}_{1,1}^{(2)}$	$\overline{\omega}_{1,1}^{(3)}$	$\overline{\omega}_{1,1}^{(4)}$	$\overline{\omega}_{1,1}^{(5)}$
n = 0.1	7.5457	33.0610	194.0023	311.1301	410.9468
n = 0.2	7.2097	27.4169	192.2516	311.3392	378.6239
n = 0.3	6.0900	25.7622	191.2195	308.6478	361.0776
n = 0.4	5.4114	22.7983	190.6838	307.9684	351.5924
n = 0.5	5.1513	19.3084	190.3310	307.1975	345.4127

Table 6: Variations in the natural frequencies of fluid-saturated porous rectangular plates with *n* under freely impermeable conditions.

$L_1/H=10$	$\overline{\omega}_{1,1}^{(1)}$	$\overline{\omega}_{1,1}^{(2)}$	$\overline{\omega}_{1,1}^{(3)}$	$\overline{\omega}_{1,1}^{(4)}$	$\overline{\omega}_{1,1}^{(5)}$
n = 0.1	8.1046	45.2650	193.9892	310.7382	410.8423
n = 0.2	6.3019	41.5898	192.1471	309.7844	377.6833
n = 0.3	5.5479	39.6392	191.2456	308.8960	361.2867
n = 0.4	5.2050	38.4804	190.6969	308.0337	351.6839
n = 0.5	5.0440	37.7265	190.3310	307.2106	345.4780

frequencies whether the upper and lower surfaces are permeable or completely impermeable, but the transverse shear stress σ_{23} and the transverse normal stress σ_{33} of the solid skeleton are influenced only slightly. Due to the strong transverse pressure gradients that occur on the beam sections and are undertaken by both the solid skeleton and pore fluid as the beam bends, the transverse bending deformation causes compression in the upper beam for $x_3 < h/2$ and tension in the lower beam for $x_3 > h/2$, which is similar to the stress distribution in a single-phase continuous elastic beam. The relationship between the total pressure and pore pressure leads to positive pore pressures in the compression zone of the upper beam and negative pore pressures in the tension zone of the lower beam, resulting in pore suction, as shown in Figure 1.

Considering different values of porosity, the variations in the solid skeleton stress, pore fluid pressure and displacements of the solid skeleton and fluid in the thickness direction are shown in Figure 2 with a frequency of $\overline{\omega} = 10$.

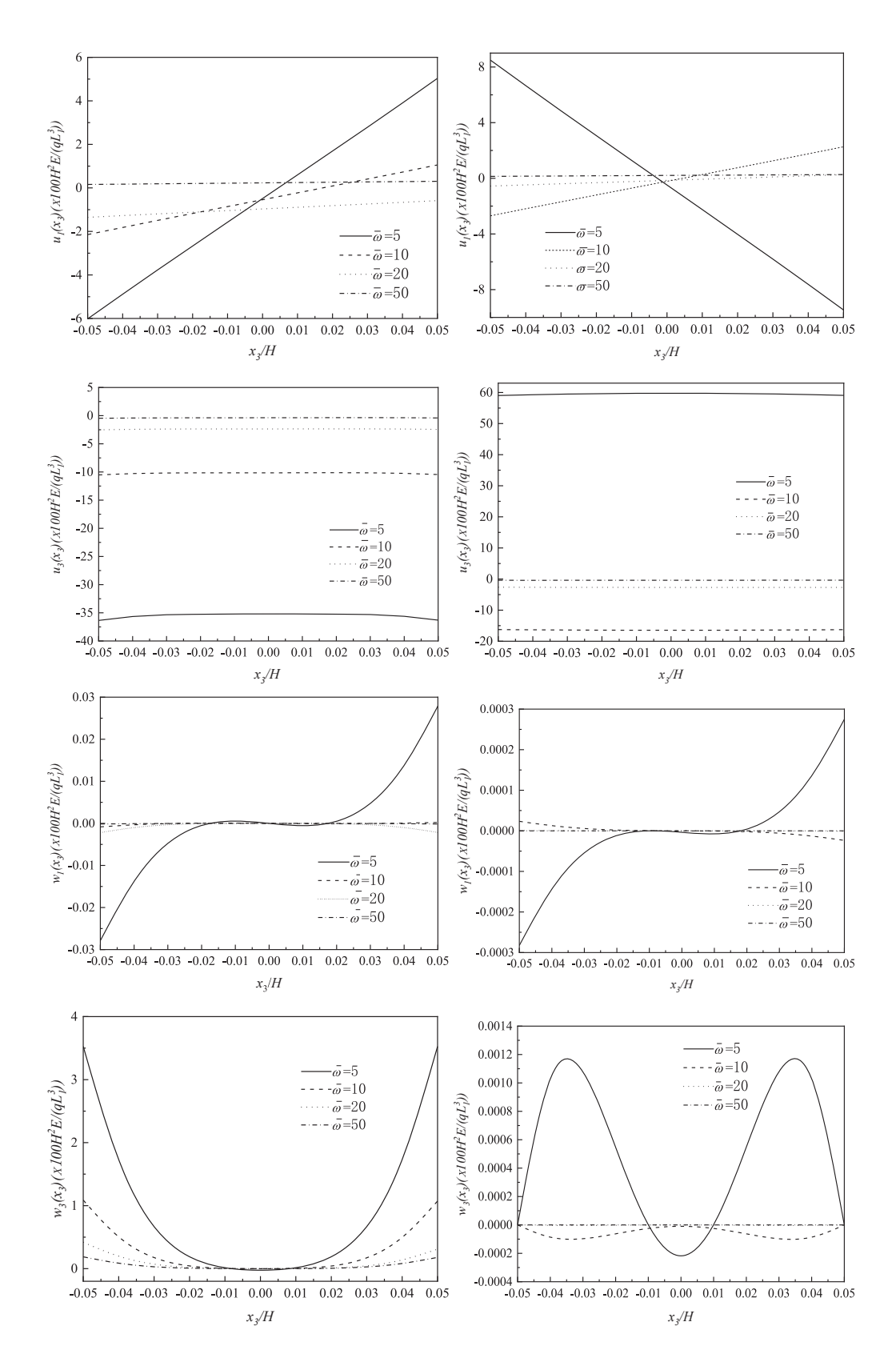


Figure 1: The variations in the solid skeleton stress, pore fluid pressure, solid skeleton displacement and pore fluid displacement in the thickness direction with $\overline{\omega}$. (1), (3), (5), (7), (9), (11), (13) and (15) are under freely permeable conditions, and (2), (4), (6), (8), (10), (12), (14) and (16) are under completely impermeable conditions.

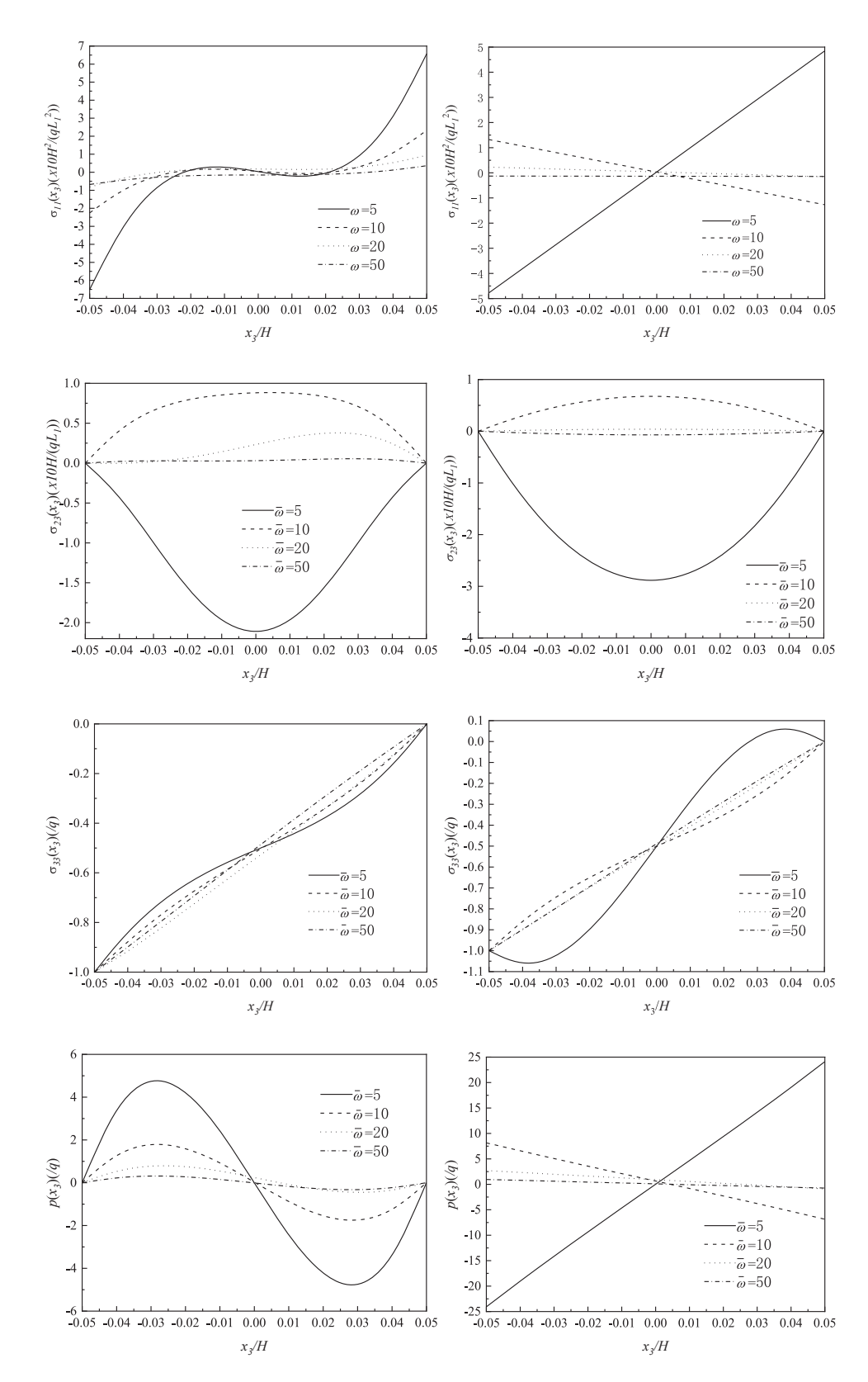


Figure 1: Continued.

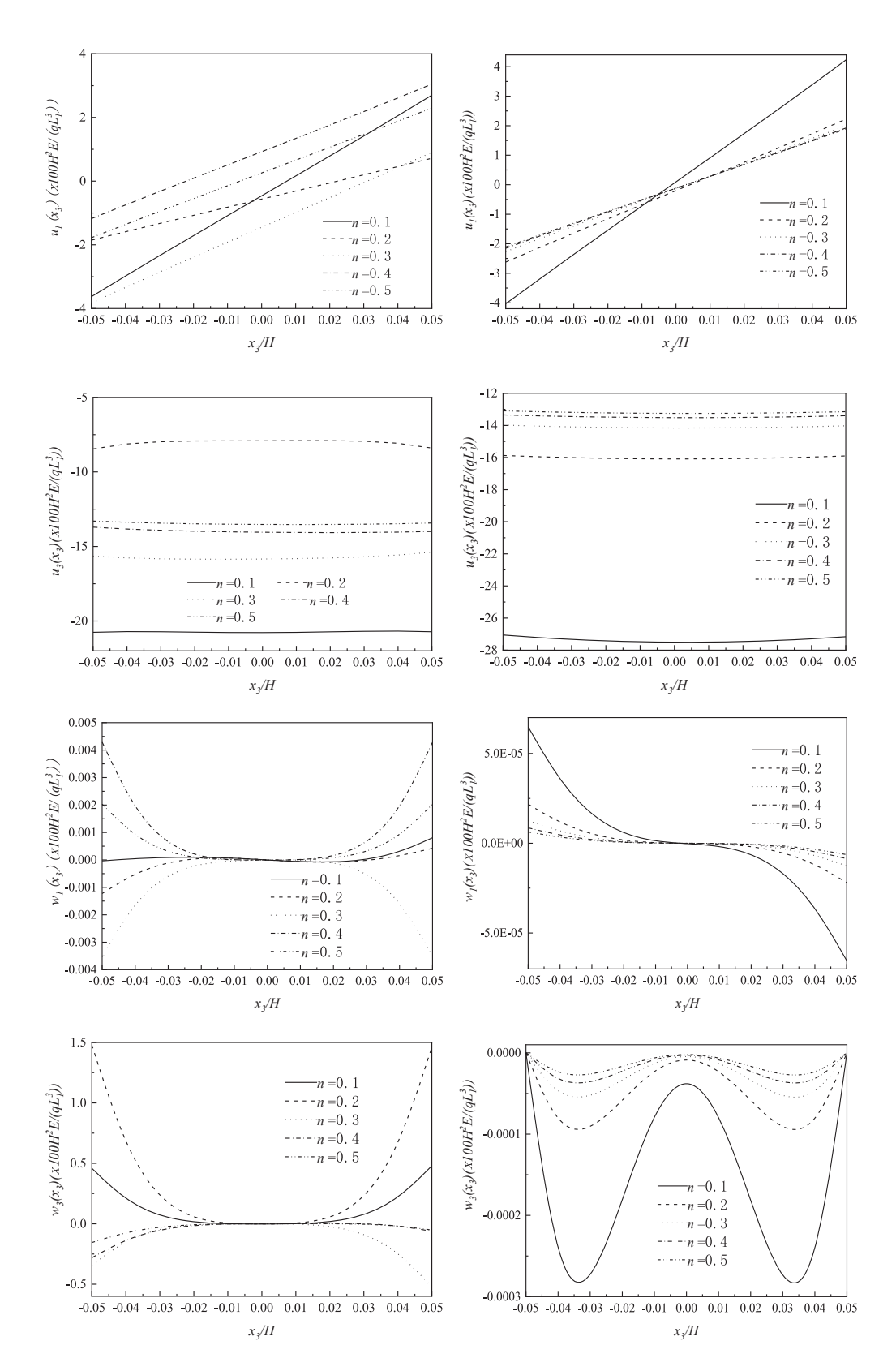


Figure 2: The variations in the solid skeleton stress, pore fluid pressure, solid skeleton displacement and pore fluid displacement in the thickness direction with n. (1), (3), (5), (7), (9), (11), (13) and (15) are under freely permeable conditions, and (2), (4), (6), (8), (10), (12), (14) and (16) are under completely impermeable conditions.

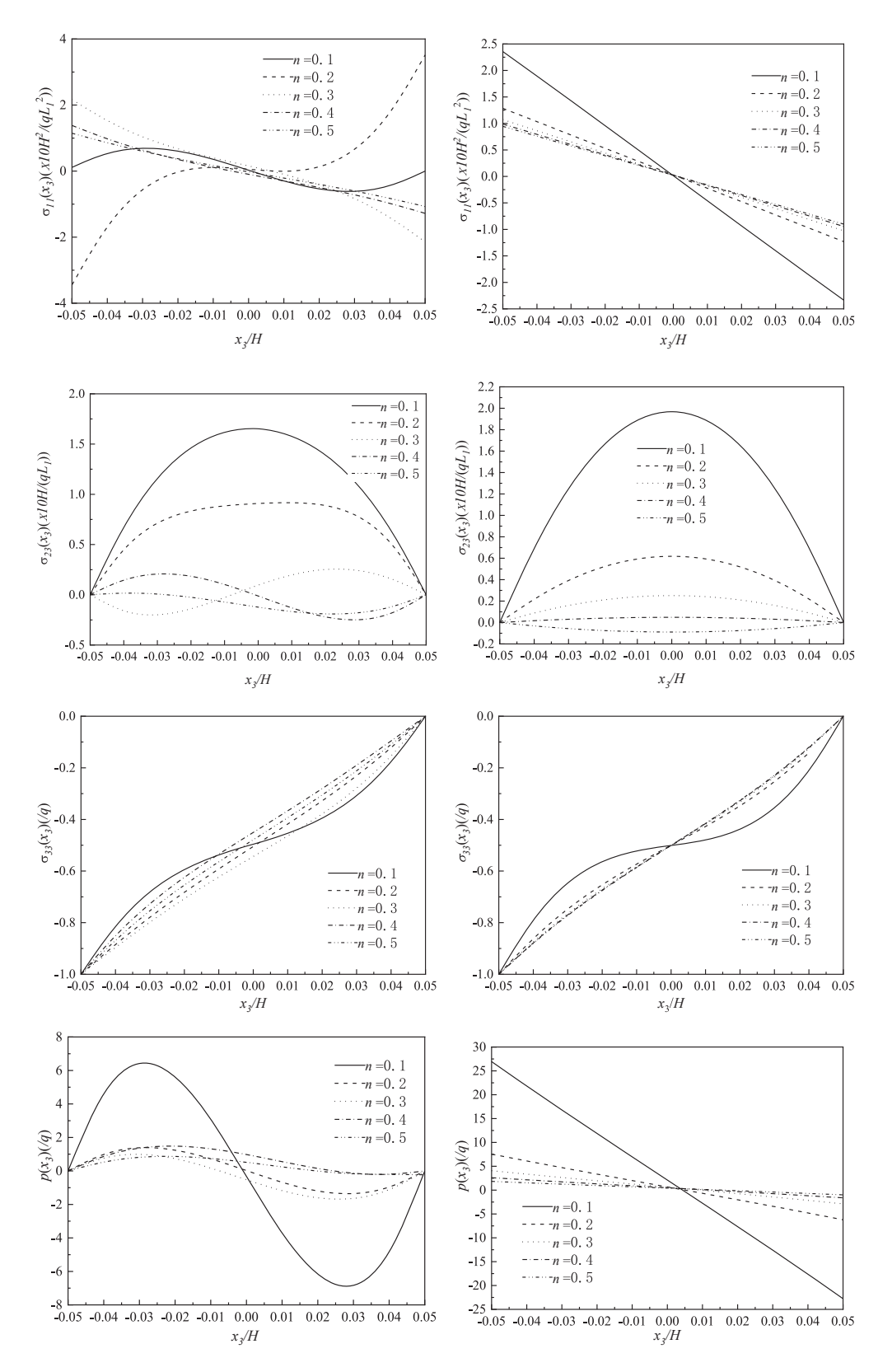


Figure 2: Continued.

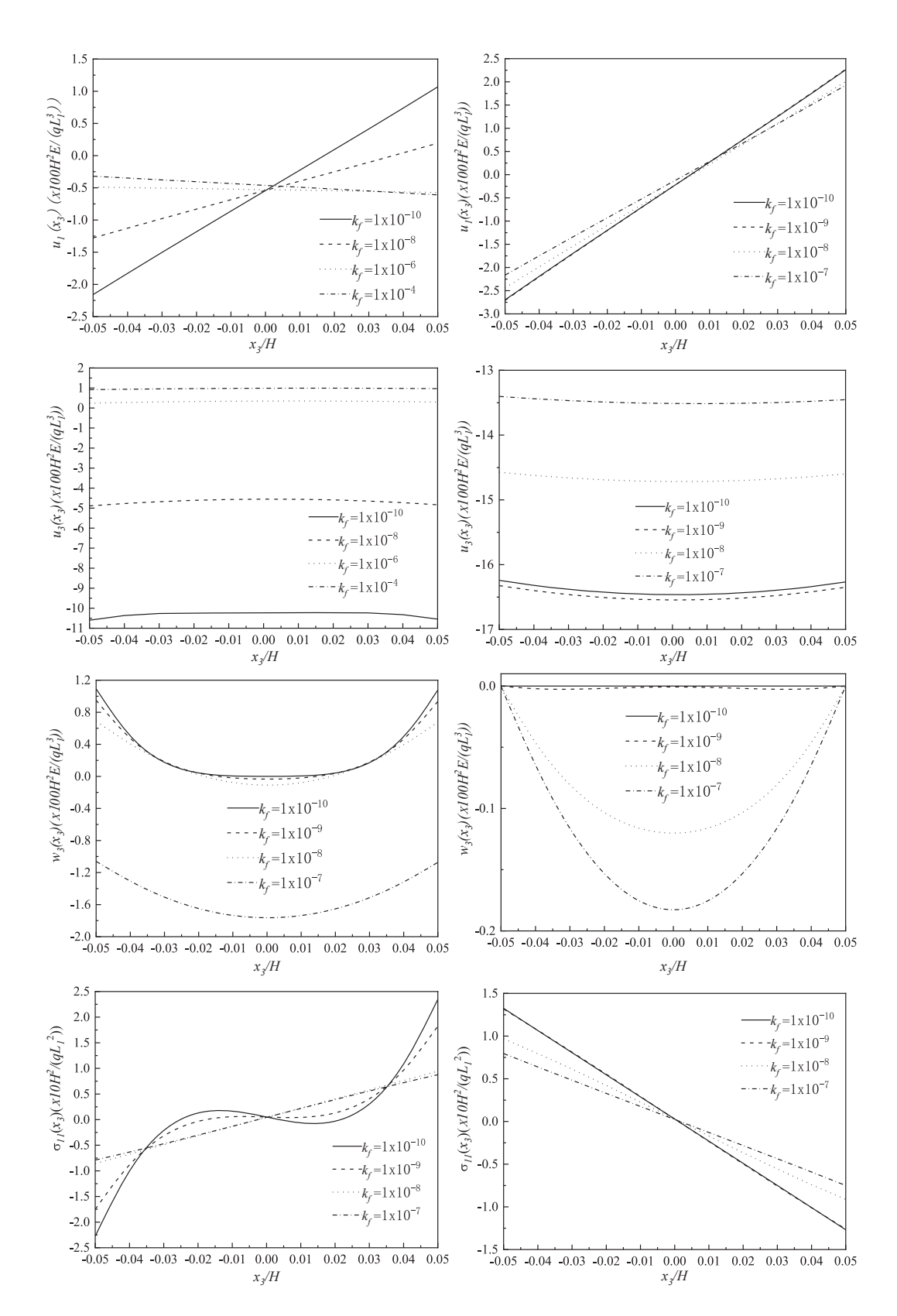


Figure 3: The variations in the solid skeleton stress, pore fluid pressure, solid skeleton displacement and pore fluid displacement in the thickness direction with k_f . (1), (3), (5), (7), (9), (11), (13) and (15) are under freely permeable conditions, and (2), (4), (6), (8), (10), (12), (14) and (16) are under completely impermeable conditions.

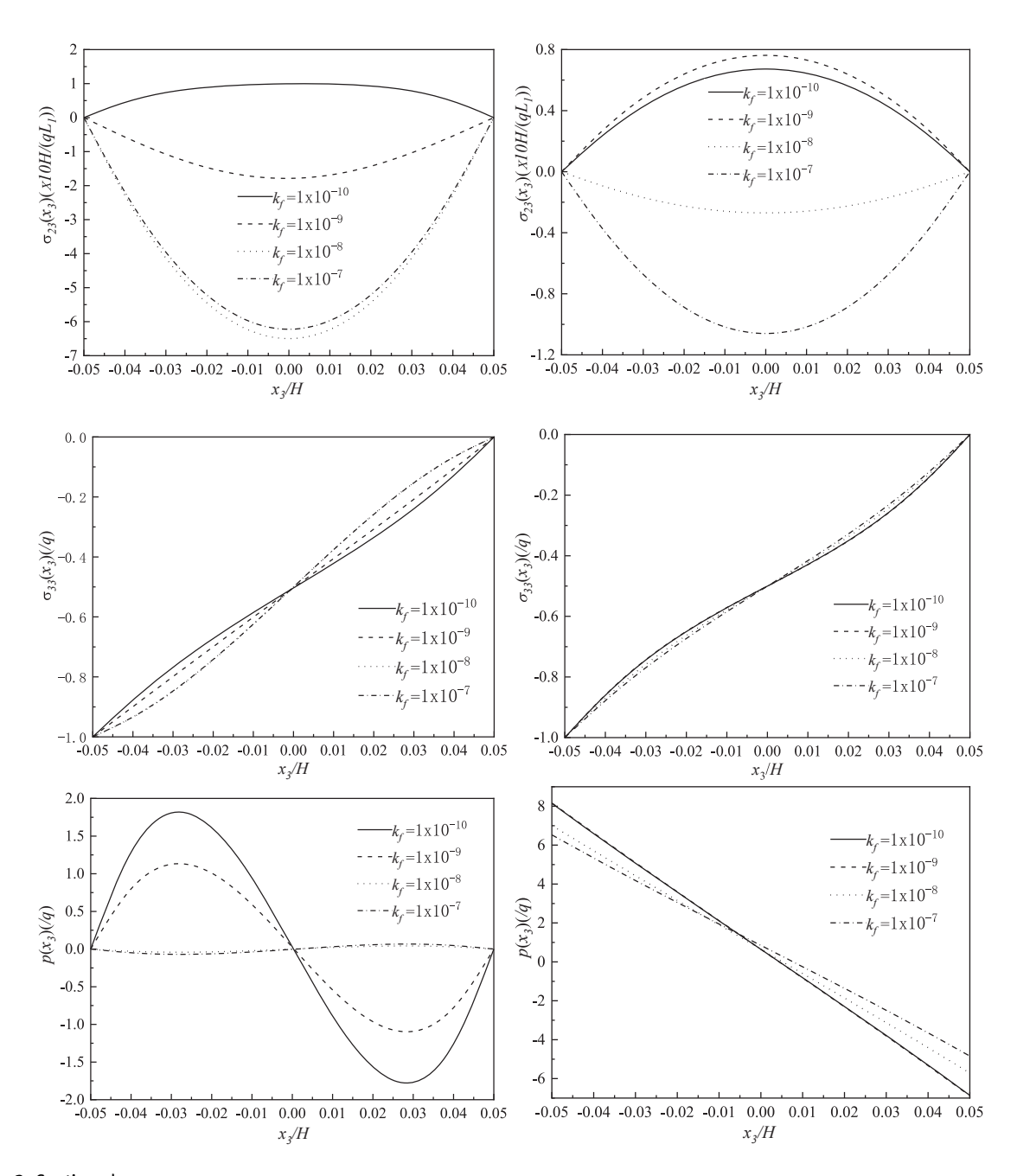


Figure 3: Continued.

The results indicate that porosity affects the solid skeleton stress, pore fluid pressure and solid skeleton and fluid displacements, although the upper and lower surface infiltration conditions have a more significant effect.

To analyse the influence of the permeability coefficient on the dynamic responses of plates, Figure 3 shows the variations in the solid skeleton stress, pore fluid pressure and solid skeleton and fluid displacements in the thickness direction. The results indicate that the permeability coefficient has an impact on the solid skeleton stress, pore fluid pressure and solid skeleton and fluid displacements. Moreover, these factors can be affected significantly by the surface infiltration conditions.

Conclusions

A series solution is presented for the dynamic responses of a simply supported fluid-saturated porous rectangular plate. Considering the compressibility of solid particles and fluid and the viscosity of pore fluid, the dynamic responses of simply supported fluid-saturated porous rectangular plates and the influence of the surface infiltration conditions, porosity and pore fluid permeability coefficient on the free vibration frequency of porous plates are discussed. Parametric studies indicate that the effect of coupling between a solid and fluid is important for increasing the frequency and must be considered in the case of dynamic responses.

contribution: Author The author has accepted responsibility for the entire content of this submitted manuscript and approved submission.

Research funding: This study was funded by Chinese Natural Science Foundation (Grant No. 51978320).

Conflict of interest statement: The author declares no conflicts of interest regarding this article.

Appendix A

$$\begin{split} Q_{11} &= \begin{bmatrix} -(\lambda + \alpha^2 M) \, \xi_1 A_{11}(x_3) - (\lambda + \alpha^2 M) \, \xi_2 A_{21}(x_3) + (\lambda + 2\mu + \alpha^2 M) \, A_{31}(x_3)' \\ -\alpha M \xi_1 B_{11}(x_3) - \alpha M \xi_2 B_{21}(x_3) + \alpha M B_{31}(x_3)' \\ Q_{12} &= \begin{bmatrix} -(\lambda + \alpha^2 M) \, \xi_1 A_{12}(x_3) - (\lambda + \alpha^2 M) \, \xi_2 A_{22}(x_3) + (\lambda + 2\mu + \alpha^2 M) \, A_{32}(x_3)' \\ -\alpha M \xi_1 B_{12}(x_3) - \alpha M \xi_2 B_{22}(x_3) + \alpha M B_{32}(x_3)' \\ -\alpha M \xi_1 B_{12}(x_3) - \alpha M \xi_2 B_{23}(x_3) + \alpha M B_{32}(x_3)' \\ -\alpha M \xi_1 B_{13}(x_3) - \alpha M \xi_2 B_{23}(x_3) + \alpha M B_{32}(x_3)' \\ -\alpha M \xi_1 B_{13}(x_3) - \alpha M \xi_2 B_{23}(x_3) + \alpha M B_{33}(x_3)' \\ Q_{13} &= \begin{bmatrix} -(\lambda + \alpha^2 M) \, \xi_1 A_{14}(x_3) - (\lambda + \alpha^2 M) \, \xi_2 A_{23}(x_3) + (\lambda + 2\mu + \alpha^2 M) \, A_{34}(x_3)' \\ -\alpha M \xi_1 B_{14}(x_3) - \alpha M \xi_2 B_{24}(x_3) + \alpha M B_{34}(x_3)' \\ -\alpha M \xi_1 B_{14}(x_3) - \alpha M \xi_2 B_{24}(x_3) + \alpha M B_{34}(x_3)' \\ Q_{15} &= \begin{bmatrix} -(\lambda + \alpha^2 M) \, \xi_1 A_{15}(x_3) - (\lambda + \alpha^2 M) \, \xi_2 A_{25}(x_3) + (\lambda + 2\mu + \alpha^2 M) \, A_{35}(x_3)' \\ -\alpha M \xi_1 B_{15}(x_3) - \alpha M \xi_2 B_{25}(x_3) + \alpha M B_{35}(x_3)' \\ Q_{16} &= \begin{bmatrix} -(\lambda + \alpha^2 M) \, \xi_1 A_{16}(x_3) - (\lambda + \alpha^2 M) \, \xi_2 A_{26}(x_3) + (\lambda + 2\mu + \alpha^2 M) \, A_{36}(x_3)' \\ -\alpha M \xi_1 B_{15}(x_3) - \alpha M \xi_2 B_{25}(x_3) + \alpha M B_{36}(x_3)' \\ Q_{17} &= \begin{bmatrix} -(\lambda + \alpha^2 M) \, \xi_1 A_{16}(x_3) - (\lambda + \alpha^2 M) \, \xi_2 A_{26}(x_3) + (\lambda + 2\mu + \alpha^2 M) \, A_{36}(x_3)' \\ -\alpha M \xi_1 B_{17}(x_3) - \alpha M \xi_2 B_{27}(x_3) + \alpha M B_{37}(x_3) \\ Q_{18} &= \begin{bmatrix} -(\lambda + \alpha^2 M) \, \xi_1 A_{18}(x_3) - (\lambda + \alpha^2 M) \, \xi_2 A_{26}(x_3) + (\lambda + 2\mu + \alpha^2 M) \, A_{36}(x_3)' \\ -\alpha M \xi_1 B_{18}(x_3) - \alpha M \xi_2 B_{28}(x_3) + \alpha M B_{36}(x_3)' \\ Q_{18} &= \begin{bmatrix} -(\lambda + \alpha^2 M) \, \xi_1 A_{18}(x_3) - (\lambda + \alpha^2 M) \, \xi_2 A_{26}(x_3) + (\lambda + 2\mu + \alpha^2 M) \, A_{36}(x_3)' \\ -\alpha M \xi_1 B_{18}(x_3) - \alpha M \xi_2 B_{28}(x_3) + \alpha M B_{36}(x_3)' \\ Q_{21} &= \mu A_{11}(x_3)' + \mu \xi_1 A_{31}(x_3), \quad Q_{22} &= \mu A_{12}(x_3)' + \mu \xi_1 A_{32}(x_3), \quad Q_{23} &= \mu A_{13}(x_3)' + \mu \xi_1 A_{33}(x_3) \\ Q_{24} &= \mu A_{14}(x_3)' + \mu \xi_1 A_{34}(x_3), \quad Q_{25} &= \mu A_{15}((x_3)' + \mu \xi_1 A_{32}(x_3), \quad Q_{26} &= \mu A_{16}(x_3)' + \mu \xi_2 A_{33}(x_3) \\ Q_{31} &= \mu A_{21}(x_3)' + \mu \xi_2 A_{31}(x_3), \quad Q_{32} &= \mu A_{23}(x_3)' + \mu \xi_2 A_{32}(x_3) - \mu A_{$$

Appendix B

$$\mathbf{Q_{ij}}(x_3) = \begin{bmatrix} Q_{11}(-H/2) & Q_{12}(-H/2) & Q_{13}(-H/2) & Q_{14}(-H/2) & Q_{15}(-H/2) & Q_{16}(-H/2) & Q_{17}(-H/2) & Q_{18}(-H/2) \\ Q_{21}(-H/2) & Q_{22}(-H/2) & Q_{23}(-H/2) & Q_{24}(-H/2) & Q_{25}(-H/2) & Q_{26}(-H/2) & Q_{27}(-H/2) & Q_{28}(-H/2) \\ Q_{31}(-H/2) & Q_{32}(-H/2) & Q_{33}(-H/2) & Q_{34}(-H/2) & Q_{35}(-H/2) & Q_{36}(-H/2) & Q_{37}(-H/2) & Q_{38}(-H/2) \\ Q_{41}(-H/2) & Q_{42}(-H/2) & Q_{43}(-H/2) & Q_{44}(-H/2) & Q_{45}(-H/2) & Q_{46}(-H/2) & Q_{47}(-H/2) & Q_{48}(-H/2) \\ Q_{11}(H/2) & Q_{12}(H/2) & Q_{13}(H/2) & Q_{14}(H/2) & Q_{15}(H/2) & Q_{16}(H/2) & Q_{17}(H/2) & Q_{28}(H/2) \\ Q_{21}(H/2) & Q_{22}(H/2) & Q_{23}(H/2) & Q_{24}(H/2) & Q_{25}(H/2) & Q_{26}(H/2) & Q_{27}(H/2) & Q_{28}(H/2) \\ Q_{31}(H/2) & Q_{32}(H/2) & Q_{33}(H/2) & Q_{34}(H/2) & Q_{35}(H/2) & Q_{36}(H/2) & Q_{37}(H/2) & Q_{38}(H/2) \\ Q_{41}(H/2) & Q_{42}(H/2) & Q_{43}(H/2) & Q_{44}(H/2) & Q_{45}(H/2) & Q_{46}(H/2) & Q_{47}(H/2) & Q_{48}(H/2) \end{bmatrix}$$

Appendix C

$$\mathbf{G_{ij}}(x_3) = \begin{bmatrix} Q_{11}(-H/2) & Q_{12}(-H/2) & Q_{13}(-H/2) & Q_{14}(-H/2) & Q_{15}(-H/2) & Q_{16}(-H/2) & Q_{17}(-H/2) & Q_{18}(-H/2) & Q_{18}(-H/2) & Q_{19}(-H/2) &$$

Appendix D

$$\mathbf{Q_{ij}'}(x_3) = \begin{bmatrix} Q_{11}(-H/2) & Q_{12}(-H/2) & Q_{13}(-H/2) & Q_{14}(-H/2) & Q_{15}(-H/2) & Q_{16}(-H/2) \\ Q_{21}(-H/2) & Q_{22}(-H/2) & Q_{23}(-H/2) & Q_{24}(-H/2) & Q_{25}(-H/2) & Q_{26}(-H/2) \\ Q_{31}(-H/2) & Q_{32}(-H/2) & Q_{33}(-H/2) & Q_{34}(-H/2) & Q_{35}(-H/2) & Q_{36}(-H/2) \\ Q_{11}(H/2) & Q_{12}(H/2) & Q_{13}(H/2) & Q_{14}(H/2) & Q_{15}(H/2) & Q_{16}(H/2) \\ Q_{21}(H/2) & Q_{22}(H/2) & Q_{23}(H/2) & Q_{24}(H/2) & Q_{25}(H/2) & Q_{26}(H/2) \\ Q_{31}(H/2) & Q_{32}(H/2) & Q_{33}(H/2) & Q_{34}(H/2) & Q_{35}(H/2) & Q_{36}(H/2) \end{bmatrix}$$

References

- [1] M. A. Biot, "Theory of propagation of elastic waves in a fluidsaturated porous solid (I.low-frequency range)," J. Acoust. Soc. Am., vol. 28, no. 2, pp. 168-178, 1956.
- [2] M. A. Biot, "Theory of propagation of elastic waves in a fluidsaturated porous solid (II.high-frequency range)," J. Acoust. Soc. Am., vol. 28, no. 2, pp. 179-191, 1956.
- [3] A. Gajo and L. Mongiovi, "An analytical solution for the transient response of saturated linear elastic porous media," Int. J. Rock Mech. Min. Sci. Geomech. Abstr., vol. 3, pp. 399-413, 1996.
- [4] X. Yang and Y. Pan, "Axisymmetrical analytical solution for vertical vibration of end-bearing pile in saturated viscoelastic soil layer," Appl. Math. Mech., vol. 2, pp. 193-204, 2010.
- [5] B. Bai, "Analytical solutions of thermal consolidation for a hollow cylinder saturated porous medium," Rock Soil Mech., vol. 32, pp. 2901-2906, 2011.
- [6] X. L. Zhou, B. Xu, J. H. Wang, and Y. L. Li, "An analytical solution for wave-induced seabed response in a multi-layered poro-elastic seabed," Ocean Eng., vol. 38, pp. 119-129, 2011.
- [7] O. C. Zienkiewicz and T. Shiomi, "Dynamic behaviour of saturated porous media: the generalized biot form formulation and its numerical solution," Int. J. Numer. Anal. Methods GeoMech., vol. 8, pp. 71-96, 1984.

- [8] Y. He and B. Han, "A wavelet finite-difference method for numerical simulation of wave propagation in fluid-saturated porous media," Appl. Math. Mech., vol. 11, pp. 1495-1504, 2008.
- [9] M. Schanz, "Poroelastodynamics: linear models, analytical solutions, and numerical methods," Appl. Mech. Rev., vol. 62,
- [10] F. X. Zhou, and Y. M. Lai, "Transient dynamic analysis of gradient fluid-saturated soil," Chin. J. Theor. Appl. Mech., vol. 44, pp. 943-947, 2012.
- [11] F. Zhou and Q. Ma, "Propagation of Rayleigh waves in fluidsaturated non-homogeneous soils with the graded solid skeleton distribution," Int. J. Numer. Anal. Methods GeoMech., vol. 40, no. 11, pp. 1513-1530, 2016.
- [12] M. Sharma, "Wave propagation in thermoelastic saturated porous medium," J. Earth Syst. Sci., vol. 117, pp. 951-958, 2008.
- [13] V. S. Polenov and A. V. Chigarev, "Wave propagation in a fluidsaturated inhomogeneous porous medium," J. Appl. Math. Mech., vol. 74, pp. 198-203, 2010.
- [14] Q. Ma and F. Zhou, "Propagation conditions of Rayleigh waves in nonhomogeneous saturated porous media," Soil Mech. Found. Eng., vol. 53, no. 4, pp. 268-273, 2016.
- [15] L. A. Taber, "A theory for transverse deflection of poroelastic plates," ASME J. Appl. Mech., vol. 59, pp. 628-634, 1992.

- [16] L. P. Li, G. Cederbaum, and K. Schulgasser, "Theory of poroelastic plates with in-plane diffusion," Int. J. Solid Struct., vol. 34, pp. 4515-4530, 1997.
- [17] P. Leclaire, K. V. Horoshenkov, and A. Cummings, "Transverse vibration of a thin rectangular porous platesaturated by a fluid," J. Sound Vib., vol. 247, pp. l-18, 2001.
- [18] P. Leclaire and K. V. Horoshenkov, "The vibrational response of aclamped rectangular porous plate," J. Sound Vib., vol. 247, pp. 19-31, 2001.
- [19] L. A. Taber, and A. M. Puleo, "Poroelastic plate and shell theories," Solid Mech. Appl., vol. 35, pp. 323-338, 1996.
- [20] P. Leclaire, K. V. Horoshenkov, and A. Cummings, "Transverse vibrations of a thin rectangular porous plate saturated by a fluid," J. Sound Vib., vol. 247, pp. 1-18, 2001.
- [21] D. D. Theodorakopoulos and D. E. Beskos, "Flexural vibrations of poroelastic plate," Acta Mech., vol. 103, nos 1-4, pp. 191-203, 1994.
- [22] Anke Busse Dipl.Ing, "Martin Schanz, Heinz antes. A poroelastic Mindlin-plate," Pammatone, vol. 3, no. 1, pp. 260-261, 2003.
- [23] Z. Feng-xi and C. Xiao-lin, "A transverse dynamic deflection model for thin plate made of saturated porous materials," Z. Naturforsch., vol. 71, no. 10, pp. 94-948, 2016.

- [24] L. Nagler and M. Schanz, "An extendable poroelastic plate formulation in dynamics," Arch. Appl. Mech., vol. 80, pp. 1177-1195, 2010.
- [25] A. S. Rezaei and A. R. Saidi, "On the effect of coupled solid-fluid deformation on natural frequencies of fluid saturated porous plates [J]," Eur. J. Mech. Solid., vol. 63, no. (Complete), pp. 99-109, 2017.
- [26] J. R. Fan, Exact Theory of Thick Laminated Plate and Shell, Beijing, Science Press, 1996.
- [27] S. V. Senthil and R. C. Batra, "Three-dimensional exact solution for the vibration of functionally graded rectangular plates," J. Sound Vib., vol. 272, pp. 703-730, 2004.
- [28] N. A. Fleck and V. S. Deshpande, "The resistance of clamped sandwich beams to shock loading," J. Appl. Mech. Trans. ASME, vol. 71, pp. 386-401, 2004.
- [29] M. T. Tilbrook, V. S. Deshpande, and N. A. Fleck, "The impulsive response of sandwich beams: analytical and numerical investigation of regimes of behaviour," J. Mech. Phys. Solid., vol. 54, pp. 2242-2280, 2006, d.
- [30] R. Rajendran and J. M. Lee, "Blast loaded plates," Mar. Struct., vol. 22, no. 2, pp. 99-127, 2009.